International Journal of Fluid Machinery and Systems
Vol. 9, No. 3, July-September 2016
DOI: http://dx.doi.org/10.5293/IJFMS.2016.9.3.265
ISSN (Online): 1882-9554

Original Paper

Energy Efficient Design of a Jet Pump by Ensemble of Surrogates and Evolutionary Approach

Afzal Husain[1], Arihant Sonawat[2], Sarath Mohan[2] and Abdus Samad[2]

[1]Department of Mechanical and Industrial Engineering, Sultan Qaboos University
Al-Khoudh, Muscat, PC-123, Oman, afzal19@squ.edu.om
[2]Department of Ocean Engineering, IITM Chennai
Chennai, 600036, India, sonawatarihant@gmail.com, sarath.gecian@gmail.com, samad@iitm.ac.in

Abstract

Energy systems working coherently in different conditions may not have a specific design which can provide optimal performance. A system working for a longer period at lower efficiency implies higher energy consumption. In this effort, a methodology demonstrated by a jet pump design and optimization via numerical modeling for fluid dynamics and implementation of an evolutionary algorithm for the optimization shows a reduction in computational costs. The jet pump inherently has a low efficiency because of improper mixing of primary and secondary fluids, and multiple momentum and energy transfer phenomena associated with it. The high fidelity solutions were obtained through a validated numerical model to construct an approximate function through surrogate analysis. Pareto-optimal solutions for two objective functions, i.e., secondary fluid pressure head and primary fluid pressure-drop, were generated through a multi-objective genetic algorithm. For the jet pump geometry, a design space of several design variables was discretized using the Latin hypercube sampling method for the optimization. The performance analysis of the surrogate models shows that the combined surrogates perform better than a single surrogate and the optimized jet pump shows a higher performance. The approach can be implemented in other energy systems to find a better design.

Keywords: Ensemble of surrogates, Multi-objective optimization, Pareto-optimal designs, Evolutionary computation. Efficiency enhancement, Jet pump.

1. Introduction

The global challenges for shortage of energy and ever-growing demands for energy consumption have encouraged researchers to develop alternative methods for energy optimization in fluid systems. The utilization of energy systems in a proper way can help reduce some of energy demands. To achieve it, the system designs should be optimized or redesigned to attain its best performance. There are several approaches available to maximize the system performance through automated optimization methods, but those are limited to less time taking simulations. The surrogate-based optimization methods, which mimic a high fidelity simulation (such as CFD simulations), are being used by several disciplines and gradually the use is increasing. The genetic algorithms are popular methods for multi-objective optimizations. The approach of combining different surrogates and genetic algorithms and analysis is not so common in academia and industries. There are ample efforts to optimize a system without optimization but introducing new concepts [1].

The fluid machinery and systems are being optimized for the last few decades. The turbomachinery systems or any piping designs are some examples. A jet pump, also known as 'ejector' or 'educator', is a very simple device, have no moving parts and used in this problem as a case study. The pump works on the Venturi effect (a special case of Bernoulli's principle). The effect states that, if no work is done on or by a flowing frictionless fluid, its total energy, which is the summation of potential, kinetic, and pressure energy remains constant. Therefore, an increase in the velocity (or the kinetic energy) results in a decrease in the pressure and vice versa. This principle is used for the entrainment and compression of low-pressure (LP) fluid to an intermediate pressure between LP and high pressure (HP) with the help of HP motive fluid. It consists of primary nozzle, secondary nozzle, mixing tube (throat) and a diffuser. The HP motive fluid passes through the primary nozzle creating a high velocity jet, generating a suction region ahead of it. This creates a favorable pressure gradient in the suction chamber causing entrainment of suction or entrained fluid. The motive and entrained fluids mix up in the mixing chamber, transferring momentum and energy. The mixture then enters the diffuser where expansion of the flow results in a static pressure rise. The pressure at the exit of the diffuser is at an intermediate level between HP and LP. These pumps have wide applications in many industries including upstream petroleum industry, chemical industry, thermal power stations, medical laboratories, air conditioning systems, mining, agriculture and nuclear reactors.

Received February 16 2016; revised June 19 2016; accepted for publication July 16 2016: Review conducted by Young Seok Choi (Paper number O16004K)
Corresponding author: Afzal Husain, Assistant Professor, afzal19@squ.edu.om

Performance characteristics of the jet pump depends mainly on its design and geometric parameters like nozzle diameters, mixing tube length and diameter, nozzle and diffuser angles and setback distance. Several researchers [2-4] carried out theoretical and experimental studies on a jet pump and suggested mathematical expressions for energy losses in the jet pump. Corteville et al. [5] identified two main reasons for the reduced usage of jet pumps i.e., the low energy efficiency of the jet pump which is usually in the range of 26-33% and also the sizing methods used for its design being considered inaccurate, incomplete and somewhat mysterious. Neto and Porto [6] conducted experiments on jet pump having area ratios of 0.25, 0.35 and 0.53 and observed that the pump with area ratio 0.35 was the most efficient among the configurations considered. Samad and Nizamuddin [7] studied the effect of geometric parameters on the pump performance by numerical simulations and found that the longer mixing tubes were favorable only at higher discharge ratios. Mikhail et al. [8] developed one-dimensional theoretical model for predicting jet pump's performance. The mixing process was investigated analytically and experimentally and empirical correlation for pressure loss coefficient was proposed.

Mallela and Chatterjee [9] carried out numerical analysis to determine the effects of area ratio, mixing tube length and shape of the driving nozzle and highlighted an improvement in efficiency with a driving nozzle of smooth curved outer wall. Kumar et al. [10] tested two-phase flow variable geometry jet pump for flash desalination system. Parametric optimization was carried out to find the optimum efficiency and corresponding distance of mixing tube from the nozzle. Chamlong et al. [11] developed a method for prediction to the optimum mixing length for driving nozzle position of the central jet pump. It was concluded that the optimum ratio of the mixing length to nozzle diameter (L_m/D_n) is 2-3.5. Several approximation methods for optimization are being used and comparative studies are presented in the literatures [12-14] which carried out numerical analysis of the jet pump and presented an improved design, which showed higher performance in terms of mass flow ratio, pressure ratio and efficiency under specified working conditions. Eves et al. [15] conducted optimization of supersonic jet pump through computational fluid dynamics (CFD) analysis and genetic algorithm to maximize the entrained flow rate under constrained primary flow; however, there is scarcity of literature on systematic multi-objective optimization of jet pump to find out the optimal performance and corresponding design parameters. A systematic optimization assisted by multiple surrogates and evolutionary algorithms drastically reduces computational expense and hastens the designing process with a reasonable fidelity.

The global Pareto-optimal front (POF) provides a comprehensive picture of optimal solutions in the design space selected for optimization. The multi-objective optimization algorithms require a large number of evaluations of performance functions to obtain global Pareto-optimal solutions in design space. There are several surrogate models which are commonly used for solving engineering problems to cut short the computational time and hasten the design optimization process [16, 17, 18]. Queipo et al. [16] presented the analysis of various surrogate models such as polynomial regression based response surface approximation (RSA), Kriging (KRG) and radial basis function (RBF) applied to liquid rocket injector design. Bellary and Samad [17] applied PRESS-based weighted average surrogate (PWS) model for centrifugal impeller design and optimization. Moon et al. [18] optimized rotating cooling channel with staggered pin fins using numerical method coupled with a surrogate model and genetic algorithm. It was observed that the predicted optimal solutions were in good agreement with the Reynolds averaged Navier-Stokes (RANS) calculated solutions. There is a wide scope available for the application of surrogates in engineering problems to enhance energy efficiency [19].

In general, the surrogate models are problem dependent and a specific surrogate model can sometimes produce erroneous results due to the lack of versatility of the models and complexity of the functions. Surrogate-modeling approach of applying multi-surrogate models concurrently reduces uncertainties arising from the typical selection of surrogate models. Goel et al. [20] developed a computational model for homogenous cryogenic cavitation employing multiple surrogates including polynomial response, radial basis neural network, Kriging and PWS models. The simultaneous use of multiple surrogate models including PWS enhances fidelity and confidence of surrogate prediction. Goel et al. [12] presented various methods of ensemble of surrogate models based on prediction error analysis of the component surrogates. Zerpa et al. [21] presented a weighted average method of ensemble of surrogates based on prediction variance. Since then researchers tried various methods of ensemble of surrogates. Husain et al. [22] carried out multi-objective optimization for dimpled channel used for turbine blade cooling. They suggested the global enhancement technique for Pareto-optimal solutions based on local resampling of multiple surrogate models [23]. Zhang et al. [24] proposed adaptive hybrid surrogate modeling for complex system behavior based on the accuracy of surrogate modeling. Higher accuracy was maintained by AHSM (Adaptive Hybrid Surrogate Modeling) for high and low dimensional models for LHS (Latin Hypercube Sampling) and Hammersley sequence sampling techniques, respectively. Lee and Choi [25] suggested pointwise ensemble of surrogates based on nearest cross validation errors. It was observed that the pointwise ensemble of surrogate-models provided more robust and accurate predictions than existing methods of ensemble of surrogate models for majority of test problems. Yin et al. [26] presented ensemble of conventional surrogate models constructed for static and dynamic LHS methods. It was found that the dynamic LHS based ensemble of surrogates provides better predictions than the static LHS based ensemble of surrogate.

In view of the contemporary approaches of optimization of energy systems, the present study employs evolutionary algorithm with the surrogate models, i.e., RSA, KRG, RBF and PWS to optimize a jet pump targeting higher efficiency and lower pressure drop. Area ratio, setback ratio and mixing tube length to diameter ratio were selected as design variables. A detailed computational approach and comparative analysis of surrogate based optimization and the flow analyses have been presented in this paper.

2. Mathematical Model

The schematic with computational domain and boundary conditions of the pump is shown in Fig. 1. The design details of the jet pump have been presented in Table 1 [27]. The RANS equations, which were solved for steady state incompressible flow can be written as:

$$\frac{\partial U_i}{\partial x_i} = 0 \qquad (1)$$

$$\rho_f U_j \frac{\partial U_i}{\partial x_j} = -\frac{\partial P}{\partial x_i} + \frac{\partial}{\partial x_j}\left\{\left(\mu_f + \mu_t\right)\left(\frac{\partial U_i}{\partial x_j} + \frac{\partial U_j}{\partial x_i}\right)\right\} \quad (2)$$

$$\rho_f Cp_f U_j \frac{\partial T}{\partial x_j} = \frac{\partial}{\partial x_j}\left\{\left(k_f + \frac{Cp_f \mu_t}{\mathrm{Pr}_t}\right)\frac{\partial T}{\partial x_j}\right\} \quad (3)$$

Here, the turbulent viscosity was modeled by *k*-*ε* model as:

$$\mu_t = C_\mu \rho_f \frac{k^2}{\varepsilon} \quad (4)$$

The equations for the turbulent kinetic energy and the dissipation rate can be written as:

$$\rho_f U_j \frac{\partial k}{\partial x_j} = \frac{\partial}{\partial x_j}\left\{\left(\mu_f + \frac{\mu_t}{\sigma_k}\right)\frac{\partial k}{\partial x_j}\right\} + P_k - \rho_f \varepsilon \quad (5)$$

$$\rho_f U_j \frac{\partial \varepsilon}{\partial x_j} = \frac{\partial}{\partial x_j}\left\{\left(\mu_f + \frac{\mu_t}{\sigma_\varepsilon}\right)\frac{\partial \varepsilon}{\partial x_j}\right\} + \frac{\varepsilon}{k}\left(C_{\varepsilon 1} P_k - C_{\varepsilon 2}\rho_f \varepsilon\right) \quad (6)$$

where,

$$P_k = \mu_t \left(\frac{\partial U_i}{\partial x_j} + \frac{\partial U_j}{\partial x_i}\right)\frac{\partial U_i}{\partial x_j} \quad (7)$$

The values of the closing coefficients are C_μ = 0.09, $C_{\varepsilon 1}$ = 1.44, $C_{\varepsilon 2}$ = 1.92, σ_k = 1.0, and σ_ε = 1.3. A variant of finite volume-based commercial code [28] which employed the coupled algebraic multi-grid method [29] was used for the flow analysis. The unstructured patch independent mesh with tetrahedral elements was generated in the computational domain as shown in Fig. 1. The RANS equations were solved for the flow analysis by applying a steady and incompressible turbulent flow. The *k*-*ε* model with scalable wall function was used for turbulence closure [30]. The upwind scheme was used to discretize the advection terms of RANS equations while high resolution scheme was used for turbulent numeric. The scalable wall function allows consistent mesh refinement and remains accurate for a fairly wide range of y+ values. The root mean square residual and mass conservation targets were set to 1×10^{-5} and 1×10^{-2}, respectively, as convergence criteria. The reference temperature and pressure were 25°C and 101 kPa, respectively. The mass flow rate was defined at the inlets of the primary and the secondary fluids, and the pressure outlet boundary condition was set at the diffuser outlet. The mass flow ratio of the primary to secondary fluid was constant, i.e., equal to one. The performance parameters for the pump are defined as:

Mass flow ratio

$$M = \frac{Q_S}{Q_P} \quad (8)$$

Pressure ratio

$$N = \frac{\text{Secondary fluid pressure rise}}{\text{Primary fluid pressure-drop}} = \frac{(P_d - P_s)}{(P_n - P_d)} \quad (9)$$

Efficiency

$$\eta = \frac{Q_S}{Q_P}\left(\frac{P_d - P_S}{P_n - P_d}\right)\times 100 = M \times N \times 100 \quad (10)$$

The mass flow ratio (M) is defined as input constraint and assigned in the flow model while the secondary fluid pressure rise (P_d - P_s) and primary fluid pressure-drop (P_n - P_d) are computed through CFD analysis.

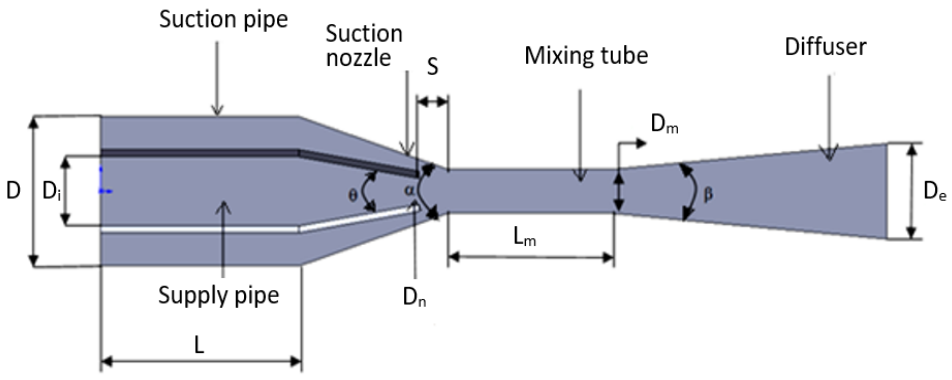

Fig. 1 Schematic of jet pump

Table 1 Geometric specifications [27]

Parameters	Dimensions
Driving nozzle exit diameter, D_n	17 mm
Setback Distance, S	22 mm
Suction nozzle inner cone angle, α	55.6°
Mixing tube diameter, D_m	32 mm
Mixing tube length, L_m	139 mm
Driving nozzle inner cone angle, θ	36.5°
Diffuser angle, β	10°
Suction pipe diameter, D	108 mm
Supply pipe diameter, D_i	50 mm
Length of supply pipe, L	154 mm
Diffuser exit diameter, D_e	69 mm

3. Optimization Model

In most of the engineering problems, high fidelity numerical or experimental solutions require a considerable amount of time varying from some seconds to days. For optimization of long time-consuming simulations, it becomes very cumbersome to obtain high fidelity solutions for a large number of designs required by a heuristic algorithm. To save the time and experimental or computational expenses, most of the time designers rely on approximate solutions obtained from low fidelity models to achieve optimal solutions. Moreover, an increase in independent design variables exponentially increases the requirement of function evaluations. However, the selection of a proper low fidelity model to a particular problem remains a challenge at large. The absence of a generalized surrogate, which can produce reliable solutions, resulted in a surge of ensemble methods as discussed during introduction without any conclusive outcomes of versatility of the approach. The PWS model [12] has been successfully applied to many of the engineering problems including heat transfer and fluid machinery. The present study critically examines several surrogates and an ensemble of surrogates to optimize the jet pump design.

Three design variables were constructed out of the several geometric parameters, which affect the performance of the jet pump, namely, area ratio (R), mixing tube length to diameter ratio (L_m/D_m) and setback ratio (S/D_m). The ranges of the variables were selected based on preliminary calculations and literature search [4-6,11,27]. Table 2 shows the details of the design variables and the ranges of the variables, which forms a design space. The efficiency of the pump is directly related to the secondary fluid pressure rise (P_d - P_s) and primary fluid pressure drop (P_n - P_d), therefore two objective functions were defined for optimization which are as follows:

$$\Delta P_1 = P_d - P_s \qquad \text{(to be maximized)} \qquad (11)$$

$$\Delta P_2 = P_n - P_d \qquad \text{(to be minimized)} \qquad (12)$$

The objective function ΔP_1 is to be maximized while ΔP_2 is to be minimized.

Table 2 Design variables and design space

Variables	LB	UB
R	0.2	0.35
L_m/D_m	0	10
S/D_m	0.2	1.5

The two objective functions were conflicting in nature; the maximization of the objective function ΔP_1 inevitably requires maximization of the objective function ΔP_2. For the discrete high fidelity numerical analysis, the design space was discretized

through LHS method [30] with 27 design points. LHS provided as many distinct levels as the design points. These levels were spaced evenly from the lower to the upper bounds of the design space. The high fidelity CFD solutions were obtained for those design variables to find out objective function responses. The design points along with the responses were used to construct the surrogate models; RSA, KRG, RBF and PWS. For details of the surrogate construction, the readers may refer to authors previous publications [13,22,23]. The cross-validation error analysis of surrogate models was performed and model predictions were validated for unsampled designs. A multi-objective optimization based on evolutionary algorithm was applied to maximize the objective function ΔP_1 and to minimize the objective function ΔP_2. A fast and elitist non-dominated sorting genetic algorithm (NSGA-II) [31] was invoked to produce Pareto-optimal solutions in the design space. NSGA-II is a methodology of simultaneously optimizing multiple objectives, which in the present study are ΔP_1 and ΔP_2. Also, it provides a set of solutions called Pareto-optimal solutions or designs for the entire design space. The procedure of the multiple surrogate assisted multi-objective optimization has been shown in Fig. 2. Further, a high fidelity CFD analysis was carried out for the selected Pareto-optimal solutions to check the fidelity of the POF and jet pump performance enhancement.

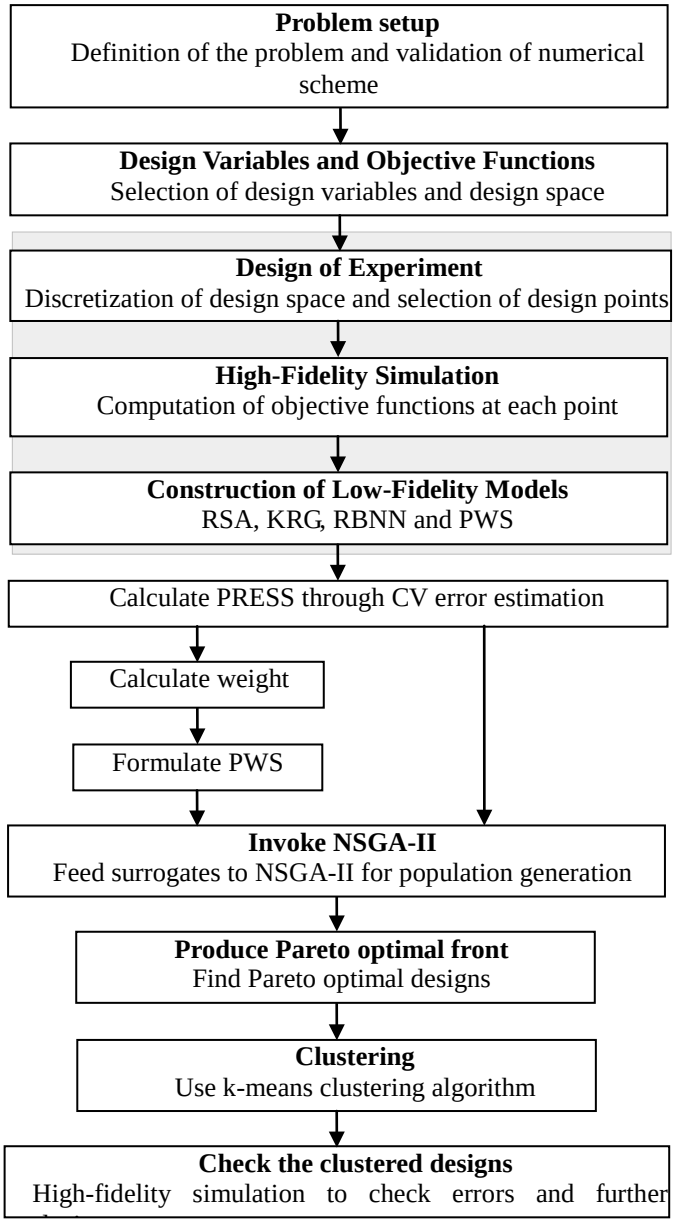

Fig. 2 Multiple surrogate assisted multi-objective optimization procedure

4. Results and Discussions

High fidelity CFD solutions are highly dependent on the grid system used to carry out the numerical analysis. In the present scheme, a grid-test was done to avoid grid dependency of CFD solutions for the efficiency and the pressure ratio as shown in Fig. 3. There is a significant change of performance parameters for the change in grid from 200,000 elements to 1,000,000 elements, but there is no significant change appears in the performance parameters with the change of grid from 1,000,000 elements to 2,000,000 elements as shown in Fig. 3. Therefore, a grid system of 1,000,000 elements has been chosen for further CFD analysis. The numerical results were validated by comparing with the experimental results of [27] and numerical results of [9], shown in Fig. 4.

The LHS produced designs were computed and analyzed for the mass flow ratio, M =1. Both the primary and the secondary working fluids were water at 25°C. The characteristic variation of both objective functions, i.e., ΔP_1 and ΔP_2, is shown in Fig. 5. The two objective functions are conflicting in nature as the increase of ΔP_1 attained at the expense of ΔP_2. The objective functions, ΔP_2 and ΔP_1 bear a nonlinear relationship within the design space discretized by LHS. The design variables and the objective functions values were used to construct the surrogate models, RSA, KRG, RBF and PWS. For the second-order curve fitting by RSA method, the values of R^2_{adj} for the two objective functions were 0.995 and 0.998, respectively. These RSA models are reliable as these values are within the limit, i.e., $0.91 < R^2_{adj} < 1$ for reasonably accurate model predictions.

The KRG models were constructed in MATLAB [32] using a toolbox [33]. The consistent performance of the KRG model depends upon the correlation function parameters that were adjusted before the models were ready for prediction at unknown location. The RBF models were constructed using the MATLAB function, *newrb*. The spread constants and error goals were adjusted carefully to achieve optimal values of errors and number of neurons.

The leave-one-out cross validation [16] was performed to assess the accuracy of each model. The cross-validation errors (E_{cv}) computed for each surrogate model for both the functions are reported in Table 3. The E_{cv} gives an idea of degree of data fitting into the approximation models or surrogates. The RSA models produced the least cross-validation errors for both functions while for KRG and RBF, these errors were comparable as shown in Table 3. The weights associated with each surrogate model were evaluated and used to form a PWS model [12]. The PWS models were formulated as:

$$\Delta P_{1,\,PWS} = w_{1,\,RSA} \times \Delta P_{1,\,RSA} + w_{1,\,KRG} \times \Delta P_{1,\,KRG} + w_{1,\,RBF} \times \Delta P_{1,\,RBF} \quad (13)$$

$$\Delta P_{2,\,PWS} = w_{2,\,RSA} \times \Delta_{P2,\,RSA} + w_{2,\,KRG} \times \Delta P_{2,\,KRG} + w_{2,\,RBF} \times \Delta P_{2,\,RBF} \quad (14)$$

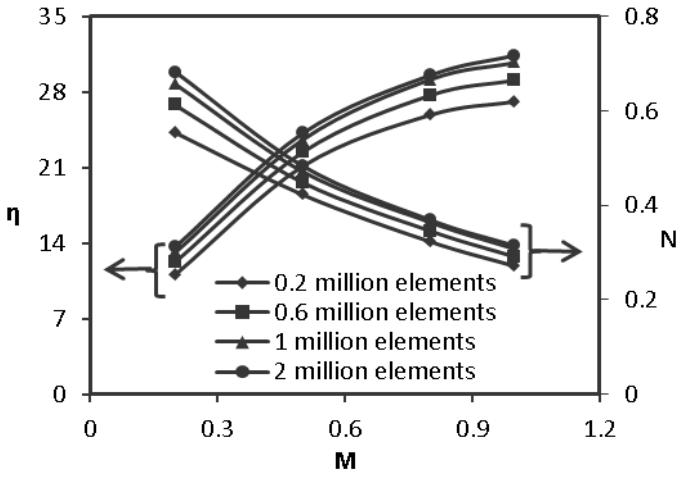

Fig. 3 Grid-test for CFD scheme

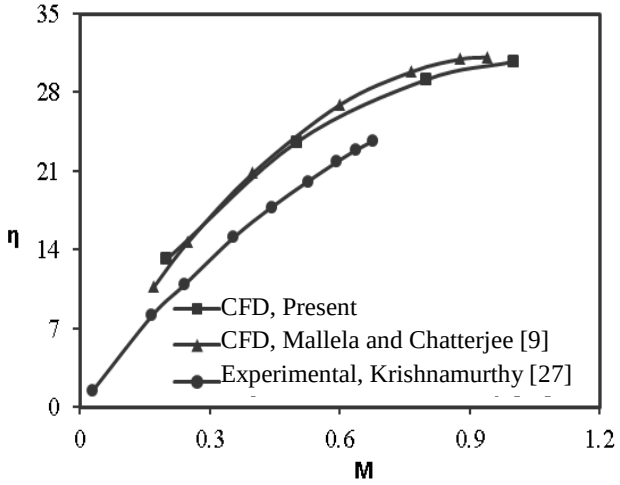

Fig. 4 Validation of CFD scheme with the existing numerical and experimental results

The least error-producing surrogate, RSA for both functions has the largest contribution to PWS construction. The KRG for function ΔP_1 and RBF for function ΔP_2 produce large errors and contributed small weights to the PWS. Further, these models were validated with high fidelity solutions for some unsampled data as shown in Table 4. Although the lower values of PRESS were associated with the RSA model for both functions, the Root Mean Square Error (RMSE) for unsampled data was the least for KRG models as shown in Table 4. This uncertainty stemmed from the inconsistent behavior of surrogate model at different regions in the design space reduces the global fidelity of the model and lays the foundation for ensemble-of-surrogates analysis. The ensemble of surrogates includes the prediction fidelities of the baseline models and unbiased Pareto-optimal solutions can be obtained. The predictions of ensemble of surrogate models, PWS, were lying between the best and worst surrogate predictions.

Table 3 Cross-validation errors and weights associated with each surrogate model to construct PWS models

Surrogate-model	E_{cv}	Weight, w
RSA	0.35	0.44
	1.13	0.52
KRG	0.71	0.22
	2.5	0.24
RBF	0.46	0.34
	2.57	0.24

Table 4 Surrogate-models validation with high fidelity CFD results

Design Variables			CFD		RSA		KRG		RBF		PWS	
R	L_m/D_m	S/D_m	Δp_1	Δp_2	Δp_1	Δp_2	Δp_1	Δp_2	Δp_1	Δp_2	Δp_1	Δp_2
0.33	2.09	0.38	8.93	26.09	8.84	25.32	8.86	24.64	8.86	25.75	8.85	25.26
0.22	5.31	1.13	18.99	75.18	17.75	70.63	18.26	73.98	18.17	73.14	18.01	72.05
0.21	4.46	1.30	20.10	83.77	19.2	80.36	19.61	81.69	19.31	81.14	19.34	80.87
0.23	1.80	0.50	17.44	60.93	17.66	61.16	17.66	61.33	15.83	54.54	17.04	59.62
Root mean square error (RMSE)					0.77	2.87	0.45	1.42	0.98	3.61	0.65	2.27

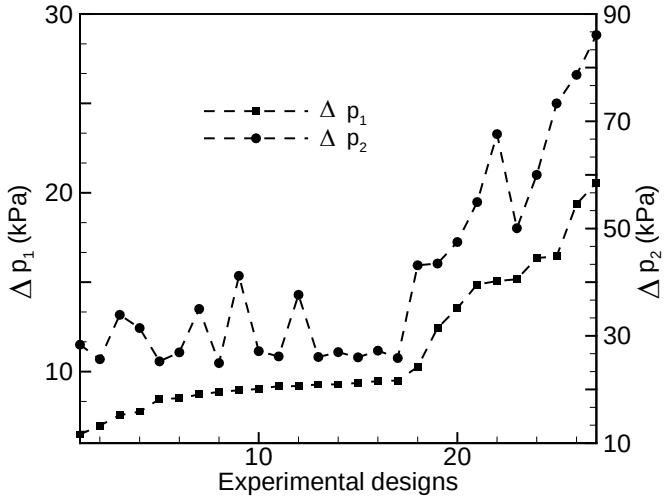

Fig. 5 Characteristic variation of the objective functions with the design points in the design space discretized by LHS

A real coded (using MATLAB) fast and elitist NSGA-II was invoked to find out Pareto-optimal designs and solutions were spread over entire design space. The various parameters related to the evolutionary algorithm were set as, N_{gen} = 250, N_{pop} = 100, P_{cvr} = 0.95 and P_{mut} = 0.05, M_{cvr} = 5, M_{mut} = 50. A hit-and-trial method was applied by changing these parameters one by one to achieve a well-spread Pareto curve within the range of design variables. The Pareto-optimal designs and solutions were obtained from all the four surrogate models as shown in Fig. 6 along with the high fidelity CFD solutions of LHS designs. It should be noted that the function ΔP_1 is maximized whereas function ΔP_2 is minimized which is evident from the POFs shown in Fig. 6. For every fixed optimal value of one objective function there is only one corresponding optimal value of other objective function for each POF. The two ends of the POF represent a set of minimum and maximum values of objective functions. With the increase of ΔP_1 there is an increase of ΔP_2, which represent a conflicting characteristic behavior of the objective functions. All the solutions on the Pareto-optimal front are non-dominating solutions and no solution is superior to other. All the surrogate models share a common functional space largely on the POFs except towards the ends. The trade-off should be noted that for an increase of ΔP_1, there is an increase of demand of ΔP_2.

The characteristic relationship between objective function and design variables for Pareto-optimal solutions can be comprehended by plotting normalized design variables against the objective functions as shown in Fig. 7. These Pareto-optimal solutions were obtained from PWS and NSGA-II, which exhibited the sensitivity of design variables along the POF. For a comprehensive multi-disciplinary multi-objective optimization, it is inevitable to understand the useful extremes of the design variables and the design space to suitably economize the optimization expense. It should be noted that the entire range of design variable α was found in the Pareto-optimal space while only part of the range for design variables β and γ were found in Pareto-optimal regime. This limits the extremes of the design space associated with Pareto-optimal solutions.

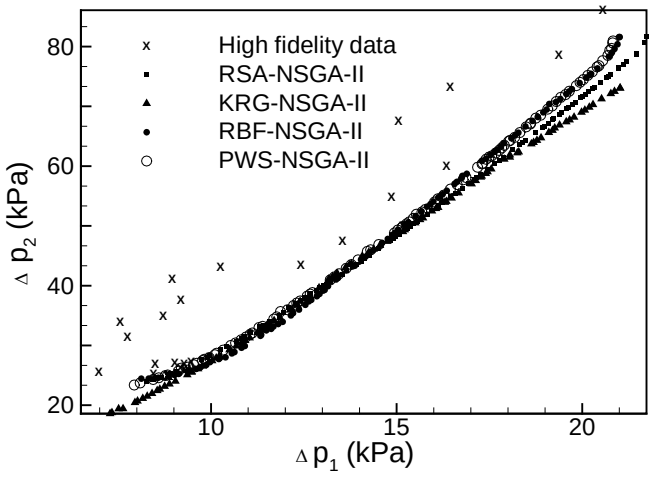

Fig. 6 Pareto-optimal fronts for various surrogate models for ΔP_1 and ΔP_2 obtained through fast and elitist NSGA-II

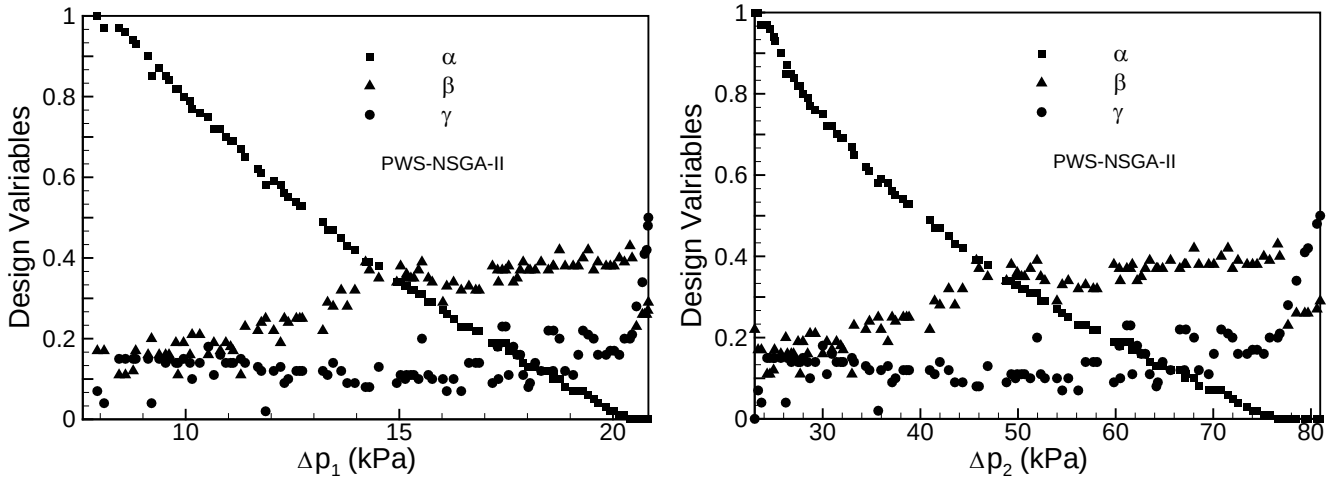

(a) (b)

Fig. 7 Distribution of design variables along the Pareto-optimal front obtained from PWS: (a) variation of design variables against ΔP_1, (b) variation of design variables against ΔP_2

The prediction fidelities of the surrogates over the POF have been examined by reproducing some of the representative Pareto-optimal designs through high fidelity CFD method. Six representative designs over the PWS-NSGA-II POFs were obtained through *k*-means clustering algorithm for fidelity analysis of PWS surrogate model. These designs were reproduced by CFD method and compared with the PWS model as shown in Fig. 8. The surrogate predicted values were close to the numerically reproduced values and the maximum error existed in PWS-NSGA-II obtained Pareto-optimal solutions were less than seven percent for each objective function. These errors are reasonable for fidelity analysis of engineering solutions. The performances of Pareto-optimal designs were further compared with the reference design. Numerical solutions were obtained for reference design as well as PODs at various mass flow ratios in the operating range as shown in Fig. 9. The ΔP_1 decreased and ΔP_2 increased monotonously with the increase of mass flow ratio for all PODs and reference design. POD-1 and POD-2 showed lower ΔP_1 and ΔP_2 while POD-4, POD-5 and POD-6 showed higher ΔP_1 and ΔP_2 than the reference design. However, POD-1, POD-2 evidently showed higher efficiency than the other PODs and reference design. The maximum efficiency shifted towards the higher values of mass flow ratio as we move from POD-1 to POD-6. The efficiency of POD-1 and POD-2 decreased at higher mass flow ratio beyond 0.8 and 1.0, respectively, due to the increased losses occurred in the mixing tube for higher S/D_m values. A maximum efficiency of 35.28% was achieved for POD-2 at mass flow ratio $M = 1$ in the present investigation.

Further, reference design is compared with the POD-1, POD-4 and POD-6 for flow field analysis as shown in Figs. 10 and 11. These figures show local distributions of turbulent kinetic energy and total pressure at the central plane. The transfer of energy from primary to secondary fluid was due to turbulent mixing of two fluid streams. Further, kinetic energy of the fluids changed into pressure head in the diffuser section. Higher mixing tube length though helped in mixing and transfer of energies of fluids, it added up into skin friction for both fluids, which consequently reduced the efficiency as evident in Fig. 11. All the PODs showed lower L_m/D_m ratio than the reference design. The lower turbulent kinetic energy at the end of mixing tube indicated higher level of mixing and transfer of energy between the primary and secondary fluid as shown in Fig. 10(c) and (d). PODs showed a gradual variation of turbulent kinetic energy and total pressure along the mixing tube and diffuser, which is expected in case of optimal designs.

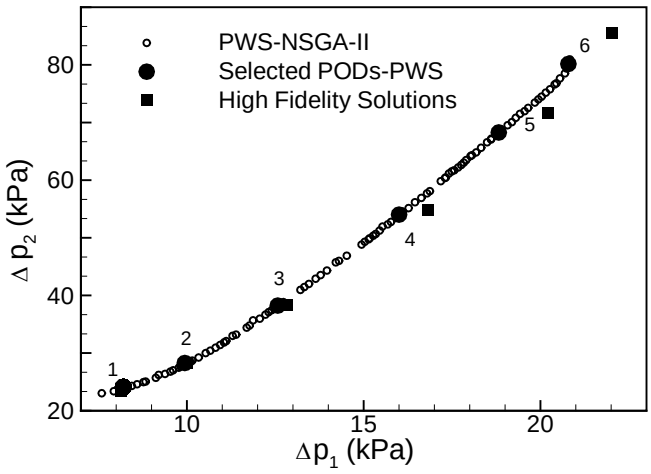

Fig. 8 Surrogate fidelity analysis Pareto-optimal solutions obtained through PWS model for the selected design (POD-1 to POD-6) along the Pareto-optimal

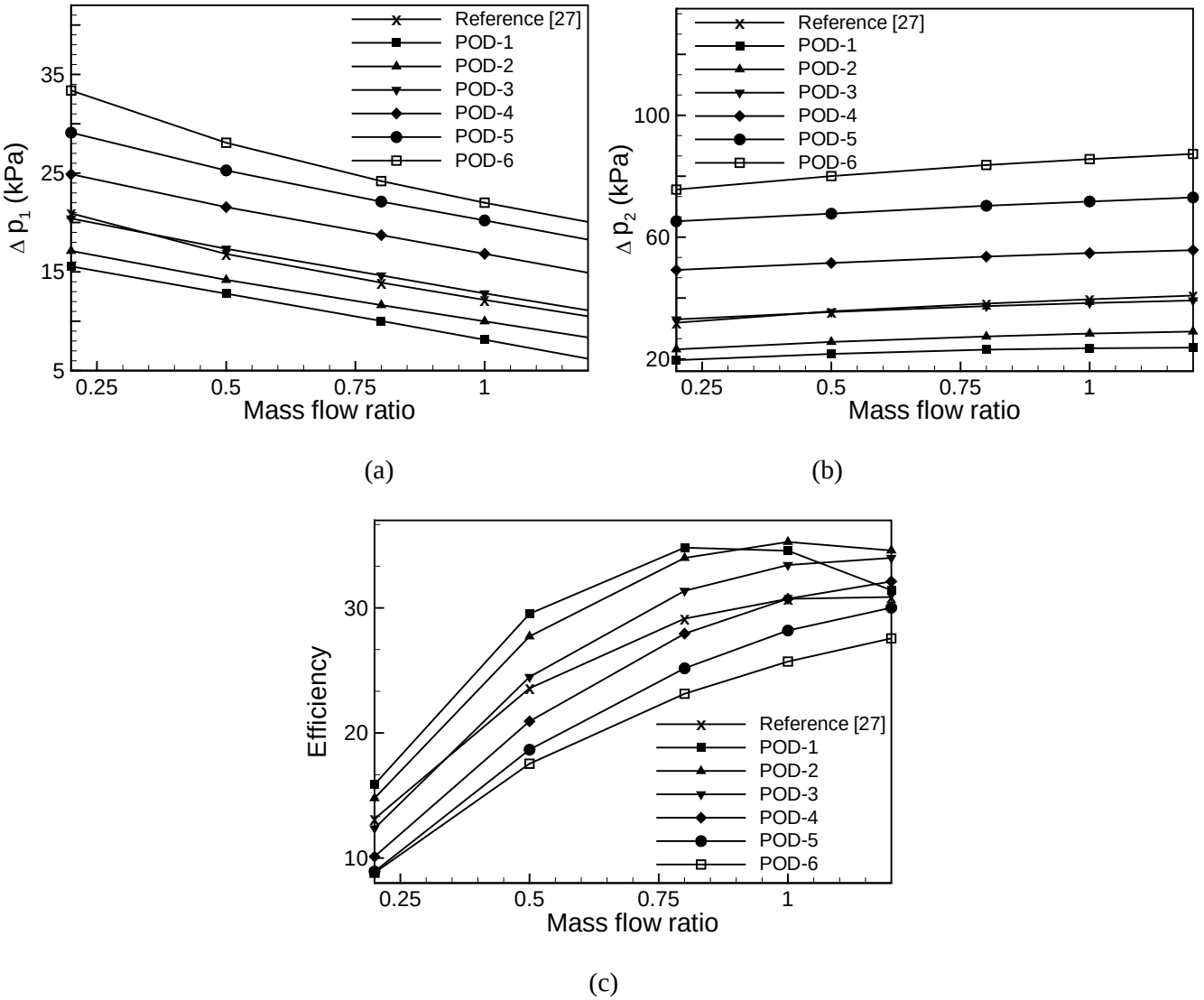

(a) (b)

(c)

Fig. 9 Comparison of PODs with Reference design [27] for: (a) Secondary fluid pressure head, (b) primary fluid pressure drop and (c) Efficiency

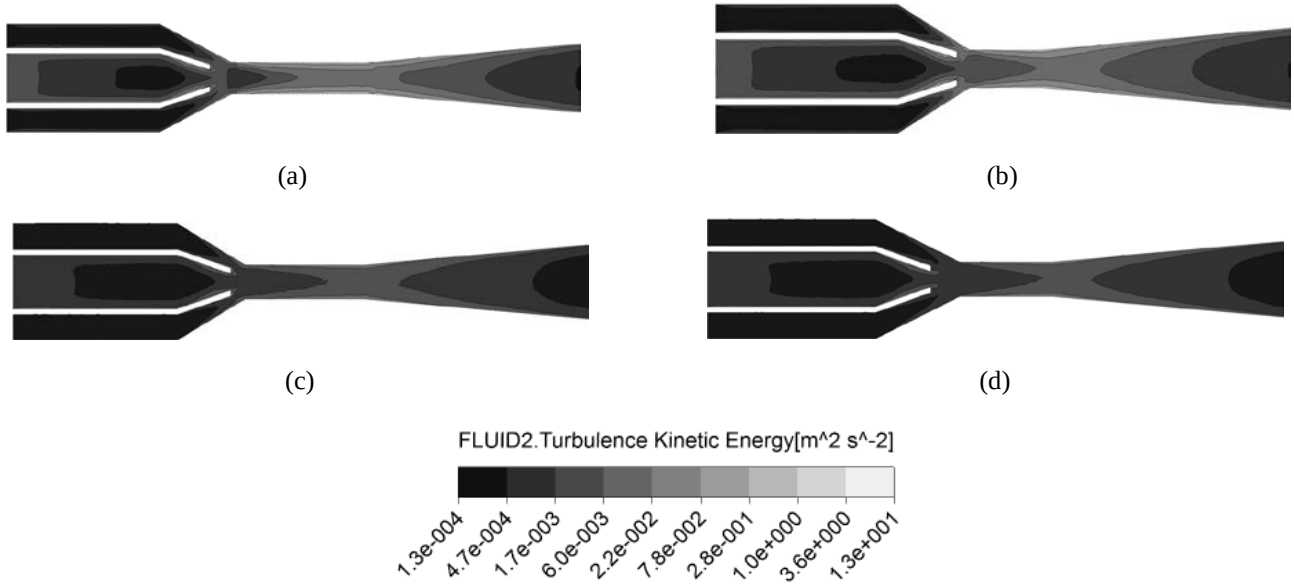

Fig. 10 Distribution of turbulent kinetic energy in the computational domain: (a) reference design [27], (b) POD-1, (c) POD-4 and (d) POD-6

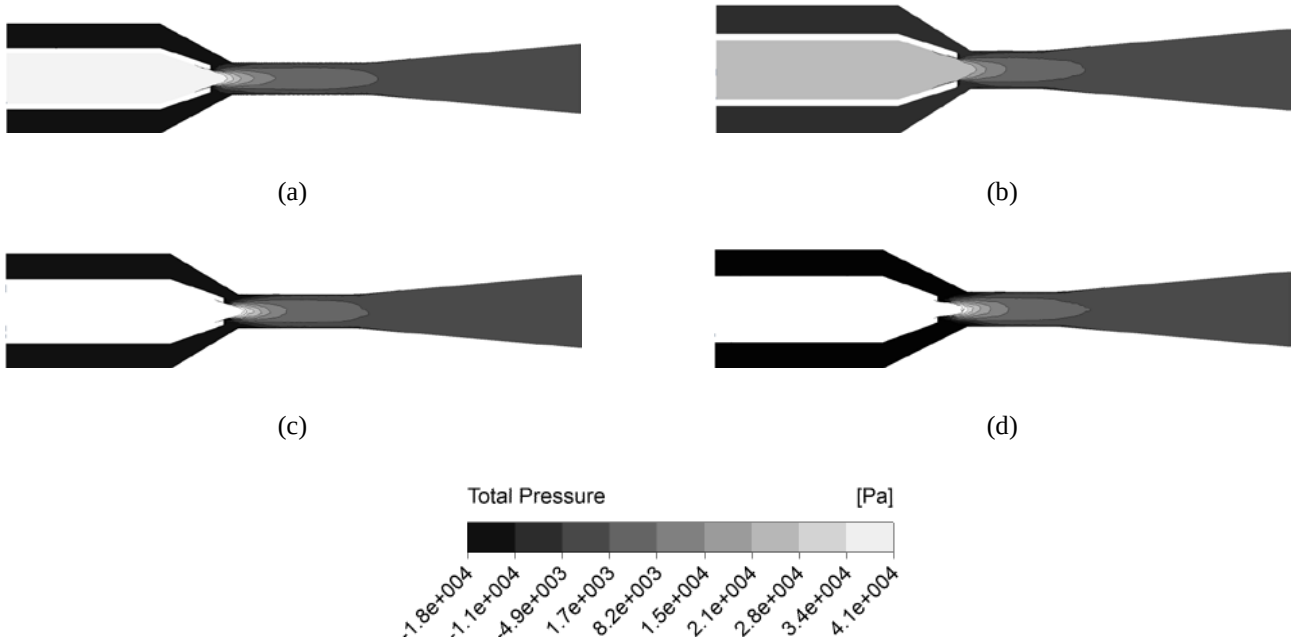

Fig. 11 Total pressure distribution in the computational domain: (a) reference design [27], (b) POD-1, (c) POD-4 and (d) POD-6

5. Conclusion

A high fidelity numerical analysis with low fidelity surrogate models and an evolutionary algorithm was implemented to enhance the performance of a jet pump. The multiple-surrogates assisted multi-objective genetic algorithm was used to enhance the jet pump performance by increasing the secondary fluid pressure head and decreasing the primary fluid pressure drop:

- The performance parameters carry a non-linear relationship with the design variables.
- The surrogate models shared a common functional space largely except at the ends.
- The Pareto-sensitivity of the objective function to design variables showed the objective functions were more sensitive to the area ratio than the other design variables.
- The PWS model carried the fidelity of the best surrogate model without being biased towards other contributing surrogate models and produced higher fidelity results. The PWS model performed better than any of the baseline model.
- The pressure head and efficiency of the jet pump were significantly enhanced through multi-objective optimization for the given primary fluid pressure drop. The efficiency of jet pump was increased by more than 4% at flow ratio M = 1.

Hence, finally it can be concluded that a multi-objective optimization gives better insight of a energy system. Implementation of multiple surrogates gives higher fidelity and approximates the POF better than a single surrogate. Hence, the approach can be used for other type of optimization of fluid machines and energy systems.

Acknowledgments

Authors acknowledge support from Indian Institute of Technology Madras, India and Sultan Qaboos University, Oman for conducting this research.

Nomenclature

	Symbols Description
D	Diameter
L	Length
w	Weight of surrogate model
M	Mass flow ratio
N	Head ratio
P	Pressure
DP	Pressure difference
R	Area ratio
S	Setback distance
N_{gen}	Number of generations
N_{pop}	Number of populations
P_{cvr}	Cross-over probability
P_{mut}	Mutation probability
M_{cvr}	Cross-over parameter
M_{mut}	Mutation parameters
C_{pf}	Specific heat of fluid
k	Turbulent kinetic energy
k_f	Conductivity of fluid
U	Mean velocity
Q_p	Flow rate primary fluid
Q_s	Flow rate secondary fluid
R^2_{adj}	R^2 adjusted
E_{cv}	Cross-validation error

	Greek Symbol
α	Inner cone angle of suction nozzle
β	Inner cone angle of diffuser
η	Efficiency
θ	Inner cone angle of driving nozzle
ε	Rate of dissipation
ρ_f	Density of fluid
μ_f	Viscosity of fluid
	Subscripts
1	Secondary fluid
2	Primary fluid
d	Diffuser outlet
KRG	Kriging
RBF	Radial basis function
RSA	Response surface approximation
m	Mixing tube
n	Driving nozzle inlet
s	Suction nozzle inlet
	Abbreviations
CFD	Computational fluid dynamics
KRG	Kriging
LHS	Latin hypercube sampling
POF	Pareto-optimal front
RBF	Radial basis function
RSA	Response surface approximation
PWS	PRESS-based weighted average surrogate
POD	Pareto-optimal Design

References

[1] Halder, P., Samad, A., Kim, J.-H., Choi, Y.-S., 2015, "High Performance Ocean Energy Harvesting Turbine Design - A New Casing Treatment Scheme," Energy, Vol. 86, pp. 219-231.

[2] Sanger, N. L., 1970, "An Experimental Investigation of Several Low-Area Ratio Water Jet Pumps," Journal of Fluids Engineering, Vol. 92, No. 1, pp. 11–20.

[3] Grupping, A. W., Coppes, J. L. R., Groot, J. G., 1988, "Fundamentals of Oil Well Jet Pumping," Journal of SPE Production Engineering, Vol. 3, No. 1, pp. 9-14.

[4] Hatzlavramidis, D. T., 1991, "Modelling and Design of Jet Pumps," SPE Production Engineering, Vol. 6, No. 4, pp. 413-419.

[5] Corteville, J. C., Ferschneider, G., Hoffmann, F.C., Valentin, E.P., 1987, "Research on Jet Pumps for Single and Multiphase Pumping of Crudes," SPE Annual Technical Conference and Exhibition, paper no. SPE-16923, pp.437-448, Dallas, Texas.

[6] Neto, I. E. L., Porto, R. M., 2004, "Performance of Low-Cost Ejectors," Journal of Irrigation and Drainage Engineering, Vol. 130, No. 2, pp. 122-128.

[7] Samad, A., Nizamuddin, M., 2013, "Flow Analyses Inside Jet Pumps Used for Oil Wells," International Journal of Fluid Machinery and Systems, Vol. 6, No. 1, pp. 1-10.

[8] Mikhail, S., Abdou, H. A. M., 2005, "Two-Phase Flow in Jet Pumps for Different Liquids," Journal of Fluids Engineering, Vol. 127, pp.1038-1042.

[9] Mallela, R., Chatterjee, D., 2011, "Numerical Investigations of the Effect of Geometry on the Performance of Jet Pump," Journal of Mechanical Engineering Science, Vol. 225, pp. 1-12.

[10] Kumar, R. S., Kumaraswamy, S., Mani, A., 2007, "Experimental Investigations on a Two-Phase Jet Pump Used in Desalination Systems," Desalination, Vol. 204, pp. 437-447.

[11] Chamlong, P., Takayama, S., Aoki, K., Nakayama, Y., 2002, "Numerical Prediction on the Optimum Mixing Throat Length for Drive Nozzle Position of the Central Jet Pump," Proceedings of 10th International Symposium on Flow Visualization, F0328, pp.1-6, Kyoto, Japan.

[12] Goel, T., Haftka, R. T., Shyy, W., Queipo, N., 2007, "Ensemble of Surrogates," Structural and Multidisciplinary Optimization, Vol. 33, No. 3, pp. 199-216.

[13] Samad, A., Kim, K.-Y., Goel, T., Haftka, R. T., Shyy, W., 2008, "Multiple Surrogate Modeling for Axial Compressor Blade Shape Optimization," Journal of Propulsion and Power, Vol. 24, No. 2, pp. 302-310.

[14] Song, X.-G., Park, J.-H., Kim, S.-G., Park, Y.-C., 2013, "Performance Comparison and Erosion Prediction of Jet Pumps by Using a Numerical Method," Mathematical and Computer Modelling, Vol. 57, No. 1–2, pp. 245–253.
[15] Eves. J., Toropov, V. V., Thompson, H. M., Kapur, N., Fan, J., Copley, D., Mincher, A., 2012, "Design Optimization of Supersonic Jet Pumps Using High Fidelity Flow Analysis," Structural and Multidisciplinary Optimization, Vol. 45, No. 5, pp. 739-745.
[16] Queipo, N. V., Haftka, R. T., Shyy, W., Goel, T., Vaidyanathan, R., Tucker, P. K., 2005, "Surrogate-Based Analysis and Optimization," Progress in Aerospace Sciences, Vol. 41, pp. 1-28.
[17] Bellary, S. A. I., Samad. A., 2014, "Improvement of Efficiency by Design Optimization of a Centrifugal Pump Impeller," ASME TURBO EXPO 2014: Turbine Technical Conference and Exposition, GT-2014, Dusseldorf, German.
[18] Moon, M. A., Husain, A., Kim. K.-Y., 2012, "Multi-Objective Optimization of a Rotating Cooling Channel with Staggered Pin Fins for Heat Transfer Augmentation," International Journal for Numerical Methods in Fluids, Vol. 68, pp. 922-938.
[19] Viana, F. A. C., Simpson, T. W., Balabanov, V., Toropov, V., 2014, "Metamodeling in Multidisciplinary Design Optimization: How Far Have We Really Come?," AIAA Journal, Vol. 52, No. 4, pp. 670-690.
[20] Goel, T., Thakur, S., Haftka, R. T., Shyy, W., Zhao, J., 2008, "Surrogate Model-Based Strategy for Cryogenic Cavitation Model Validation and Sensitivity Evaluation," International Journal for Numerical Methods in Fluids, Vol. 58, pp. 969-1007.
[21] Zerpa, L. E., Queipo, N. V., Pintos, S., Salager, J. L., 2005, "An Optimization Methodology of Alkaline-Surfactant-Polymer Flooding Processes Using Field Scale Numerical Simulation and Multiple Surrogates," Journal of Petroleum Science and Engineering, Vol. 47, pp. 197-208.
[22] Husain, A., Lee, K.-D., Kim, K.-Y., 2011 "Enhanced Multi-Objective Optimization of a Dimpled Channel Through Evolutionary Algorithms and Multiple Surrogate Methods," International Journal for Numerical Methods in Fluids, Vol. 66, pp. 742-759.
[23] Husain, A., Kim, K.-Y., 2010, "Enhanced Multi-Objective Optimization of a Microchannel Heat Sink through Evolutionary Algorithm Coupled with Surrogate Models," Applied Thermal Engineering, Vol. 30, pp. 1683-1691.
[24] Zhang, J., Chowdhury, S., Zhang, J., Messac, A., Castillo, L., 2013, "Adaptive Hybrid Surrogate Modeling for Complex Systems," AIAA Journal, Vol. 51, No. 3, pp. 643-656.
[25] Lee, Y., Choi, D.-H., 2014, "Pointwise Ensemble of Meta-Models using ν nearest Points Cross-Validation," Structural and Multidisciplinary Optimization, Vol. 50, No. 3, pp. 383-394.
[26] Yin, H., Wen, G., Fang, H., Qing, Q., Kong, X., Xiao, J., Liu, Z., 2014, "Multiobjective Crashworthiness Optimization Design of Functionally Graded Foam-Filled Tapered Tube Based on Dynamic Ensemble Metamodel," Materials and Design, Vol. 55, pp. 747-757.
[27] Krishnamurthy, P., 1975, "Design, Fabrication and Testing of Multiple Nozzle Jet Pump," M.Tech Report, Hydro-Turbomachines Laboratory, Department of Mechanical Engineering, IIT Madras.
[28] ANSYS., 2010, "ANSYS-CFX v13.0 manual," ANSYS Inc.
[29] Raw, M., 1996, "Robustness of Coupled Algebraic Multigrid for the Navier–Stokes Equations," AIAA 34th Aerospace Sciences Meeting and Exhibit, AIAA 96-0297, Reno, USA.
[30] Launder, B. E., and Spalding, D. B., 2001, "Lectures in Mathematical Models of Turbulence," Academic Press Inc, London, England.
[31] Deb, K., 2001, "Multi-Objective Optimization using Evolutionary Algorithms," 1st ed. John Wiley and Sons, New York.
[32] MATLAB., 2004, "MATLAB The Language of Technical Computing," The MathWorks Inc.
[33] Lophaven, S. N., Nielsen, H. B., Sondergaard, J., 2002, "A MATLAB Kriging Toolbox," Technical Report IMM-TR2002-12, Technical University of Denmark, Denmark.